Available at www.sciencedirect.com

ScienceDirect

journal homepage: www.elsevier.com/locate/he

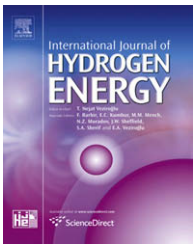

Effects of hydrogen addition on the propagation of spherical methane/air flames: A computational study

*Zheng Chen**

State Key Laboratory for Turbulence and Complex Systems (SKLTCS), College of Engineering, Peking University, Beijing 100871, China

ARTICLE INFO

Article history:
Received 12 April 2009
Received in revised form
1 June 2009
Accepted 1 June 2009
Available online 21 June 2009

Keywords:
Hydrogen
Methane
Propagating spherical flame
Laminar flame speed
Markstein length

ABSTRACT

A computational study is performed to investigate the effects of hydrogen addition on the fundamental characteristics of propagating spherical methane/air flames at different conditions. The emphasis is placed on the laminar flame speed and Markstein length of methane/hydrogen dual fuel. It is found that the laminar flame speed increases monotonically with hydrogen addition, while the Markstein length changes non-monotonically with hydrogen blending: it first decreases and then increases. Consequently, blending of hydrogen to methane/air and blending methane to hydrogen/air both destabilize the flame. Furthermore, the computed results are compared with measured data available in the literature. Comparison of the computed and measured laminar flame speeds shows good agreement. However, the measured Markstein length is shown to strongly depend on the flame radii range utilized for data processing and have very large uncertainty. It is found that the experimental results cannot correctly show the trend of Markstein length changing with the hydrogen blending level and pressure and hence are not reliable. Therefore, the computed Markstein length, which is accurate, should be used in combustion modeling to include the flame stretch effect on flame speed.

1. Introduction

Environmental regulations and energy diversity produce an urgent need to develop and use clean alternative fuels. Natural gas, which offers considerable economic and environmental advantages, resulting from improved efficiency, availability, and pollutant emissions [1], is currently one of the most promising clean alternative fuels. However, the low ignitability and low flame speed of methane (the main component of natural gas) pose great challenges for its utilization in combustion engines [1]. To solve this problem, one of the effective methods is to add more reactive fuels such as hydrogen to promote ignition and enhance flame speed [2]. In fact, recent studies [3,4] have already demonstrated the promising performance of adding hydrogen to methane in internal combustion engines and indicated a definite advantage in blending hydrogen.

In order to understand the combustion properties of hydrogen enriched methane and to develop high-performance combustion engines utilizing hydrogen blended natural gas, fundamental investigation on the ignition, flame propagation, flame stability, and extinction of methane/hydrogen dual fuel is essential. A number of experimental and numerical studies have been conducted for hydrogen enriched methane. Yu et al. [2] showed that blending of hydrogen causes an increase in the laminar flame speed due to the increase of flame temperature and decrease of activation energy. Fotache et al. [1] found that hydrogen addition can significantly improve methane ignition

* Tel.: +86 (10)6275 6559; fax: +86 (10)6275 7532.
E-mail address: cz@pku.edu.cn
0360-3199/$ – see front matter
doi:10.1016/j.ijhydene.2009.06.001

through a mechanism of increased radical production. Experiments [5–8] on propagating spherical methane/hydrogen/air flames revealed that adding hydrogen will decrease the Markstein length and hence destabilize the flame propagation. Using counterflow premixed flames, Jackson et al. [9] found that blending of hydrogen to methane/air has a significant effect in increasing the extinction strain rate. More recently, numerical simulation of premixed planar flames [10,11] and counterflow flames [12–14] showed that hydrogen addition to methane can increase the laminar flame speed and greatly improve the flammability limits.

In this study, we will focus on the effects of hydrogen addition on propagating methane/air flames. It is well known that flame properties such as flame speed and flame stability depend on the overall activation energy and the Lewis number [15,16]. Kinetic coupling will result in a dramatic change in the overall activation energy with hydrogen addition to methane. Moreover, hydrogen has a molecular weight much lower than methane so that the Lewis number of methane/air flames is significantly changed with hydrogen addition. The dependence of the stretched flame speed and flame stability on activation energy and Lewis number is characterized by the so-called Markstein length [15–17]. Therefore, it is of interest to investigate how the Markstein length depends on the hydrogen content in the methane/hydrogen dual fuel. Furthermore, certain current models of premixed turbulent combustion use the Markstein length as the basic input physicochemical parameter [18]. For this reason, finding the Markstein length is also important for turbulent combustion modeling of hydrogen enriched methane/air flames.

Another focus of this study is to compare the computed results with measured data in the literature and to provide accurate laminar flame speed and Markstein length of methane/hydrogen/air flames. Recently, the method utilizing propagating spherical flames has become one of the most favorable methods for measuring laminar flame speed and Markstein length (see Ref. [19] and references therein). Measured data for methane/air, hydrogen/air, and methane/hydrogen/air flames using this method are available in the literature [5–8]. The accuracy of the measured laminar flame speed using propagating spherical flames has been systematically studied [19–21] and also confirmed by comparison among measured results from different researchers [6,22–24]. However, there are few studies on the accuracy of the measured Markstein length using propagating spherical flames and the reliability of measured data remains unclear. As will be shown later, the relative difference among the measured Markstein length by different researchers [6–8,22,23,25] is in the order of 100% for methane/air and methane/hydrogen/air flames. Such large uncertainty makes the measured Markstein length not useful. In this study, the cause for the uncertainty/inaccuracy in the measured Markstein length will be investigated and an accurate Markstein length from numerical simulations will be presented.

2. Numerical method and formulation

The computational configuration is a propagating premixed spherical flame in a closed chamber, which is the same as that employed in experiments [5–8]. A time-accurate and space-adaptive numerical solver for Adaptive Simulation of Unsteady Reactive Flow, A-SURF, has been developed to conduct high-fidelity numerical simulation of one-dimensional propagating spherical flames under a broad range of pressures. A-SURF has been successfully used and validated in a series of studies [19–21,26,27]. Details on the governing equations, numerical schemes, and code validation can be found in Refs. [20,27] and hence are only briefly described below.

For a propagating spherical flame in a closed chamber, due to the pressure change and the pressure-induced compression wave, the unsteady compressible Navier–Stokes equations for multi-component reactive flow are solved in A-SURF. The finite volume method is employed for discretizing the conservation governing equations in the spherical coordinate. The second-order-accurate Strang splitting fractional-step procedure [28] is utilized to separate the time evolution of the stiff reaction term from that of the convection and diffusion terms. In the first fractional step, the non-reactive flow is solved. The Runge–Kutta, central difference, and MUSCL-Hancock schemes, all of second-order accuracy, are employed for the calculation of the temporal integration, diffusive flux, and convective flux, respectively. The chemistry is solved in the second fractional step by using the VODE solver [29]. The full methane–air reaction mechanism (GRI-MECH 3.0) [30] including the NOx chemistry is used in the present study. The detailed chemistry as well as thermodynamic and transport properties is evaluated using the CHEMKIN and TRANSPORT packages [31,32] interfaced with A-SURF. In order to maintain adequate numerical resolution of the moving flame front, a multi-level, dynamically adaptive mesh refinement algorithm has been developed. Nine grid levels are utilized in this study and the moving reaction zone is always fully covered by the finest meshes of 8 μm in width. The grid convergence is tested to ensure numerical accuracy of the solutions.

Propagating spherical flames of mixtures ranging in composition from pure methane/air to pure hydrogen/air and from fuel lean to fuel rich are studied. The initial fresh mixture composition is specified according to $\varphi[(1-a)CH_4 + aH_2]+(2-1.5a)[O_2 + 3.76N_2]$, where φ is the effective equivalence ratio ($\varphi = 0.8$, 1.0, and 1.2 for fuel lean, stoichiometric, and fuel rich, respectively) and a is the volume percentage of hydrogen in the methane/hydrogen dual fuel ($a = 0$, 0.2, 0.4, 0.6, 0.8, 1). In all simulations, the spherical chamber radius is set to be $R_w = 100$ cm (i.e. the computational domain is $0 \le r \le 100$ cm) and only the flame trajectory data with flame radius less than 5 cm are utilized for extrapolating the laminar flame speed and Markstein length. Therefore, both pressure increase (<0.15‰) and compression-induced flow [19] are negligible. The flame is initiated by a small hot pocket (1 ~ 2 mm in radius) of burned product surrounded by fresh mixture at room temperature ($T_u = 298$ K) and initially specified pressure ($P = 0.8$, 1, or 2 atm). Zero-gradient conditions are enforced at both inner ($r = 0$) and outer ($r = R_w$) boundaries. To exclude the effects of ignition on flame propagation [20,33], only the flame trajectory data with flame radius larger than 1 cm is used for data processing. Since the effects of radiative loss [25,34] can be neglected for most mixtures such as hydrogen/air and methane/air not close to

flammability limits and without CO_2 dilution [27], radiation is not included in simulations.

From the flame front history, $R = R(t)$, defined as the position where maximum heat release occurs in simulations, the laminar flame speed and Markstein length can be obtained (the details of this method can be found in Refs. [19,25,33,35]). There are various methods found in the literature for relating the stretch rate and the stretched flame speed such that the unstretched laminar flame speed and Markstein length can be extracted as described in Refs. [25,33,35]. In the present study, we will use the definition of Clavin [15]

$$S_b = S_b^0 - L_b K \quad (1)$$

where S_b^0 and S_b are respectively the unstretched and stretched flame speed with respect to the burned mixture, L_b the Markstein length relative to burned gas, and K the flame stretch rate. For outwardly propagating spherical flames, the stretch rate is $K = 2R^{-1}dR/dt$. When the compression-induced flow [19] is negligible, the burned gas inside the spherical flame front is static and hence the stretched flame speed with respect to burned gas is equal to the propagating speed of the flame front, i.e. $S_b = dR/dt$. Therefore, according to Eq. (1), S_b^0 and L_b can be obtained from the linear extrapolation based on the plot of S_b–K, where both S_b and K are calculated from the flame front history, $R = R(t)$. Knowing S_b^0, the unstretched laminar flame speed relative to the unburned mixture, S_u^0, can be deduced through mass conservation: $S_u^0 = \sigma S_b^0$, where $\sigma = \rho_b/\rho_u$ is the density ratio between the burned and unburned mixtures.

The normalized form of Eq. (1) is written as

$$S_b/S_b^0 = 1 - Ma'Ka \quad (2)$$

where $Ka = K\delta^0/S_u^0$ is the Karlovitz number and $Ma' = \sigma L_b/\delta^0$ is the Markstein number. The laminar flame thickness δ^0 is defined as $\delta^0 = (T_{ad} - T_u)/(dT/dx)_{max}$ based on the temperature profile of the planar flame structure [16]. The Karlovitz number represents the normalized stretch rate and the Markstein number represents the sensitivity of the flame speed to stretch rate [15]. It is noted that the Markstein length relative to burned gas instead of unburned gas is adopted in this study because the burned Markstein length is relatively insensitive to the choice of the reference surface and is reported by most of the experimental studies on propagating spherical flames [25].

3. Results and discussions

3.1. Results for atmospheric methane/air flames

Fig. 1 shows the evolution of the temperature profile and total heat release rate profile of a propagating stoichiometric methane/air flame initially at room temperature and atmospheric pressure. The flame temperature and maximum heat release rate are shown to continuously increase during flame propagation. This is because the Lewis number of the stoichiometric methane/air mixture is slightly higher than the critical Lewis number for which the flame stretch effect is zero, and consequently the positive flame stretch weakens the flame and makes the flame temperature and total heat release rate both lower than those of the unstretched planar flame [16]. During the propagation, the stretch rate (which is proportional to the inverse of flame radius) continuously decreases and so does the stretch effect. As a result, the larger the flame radius, the smaller the stretch effect and hence the closer the flame temperature and total heat release rate to those of the unstretched planar flame.

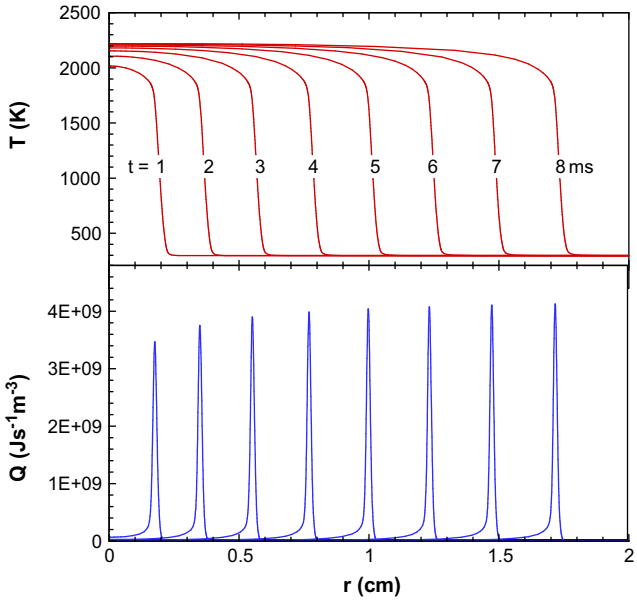

Fig. 1 – Profiles of temperature and total heat release rate at different times of a propagating stoichiometric methane/air flame at atmospheric pressure.

The variation of the stretched flame speed with flame radius and stretch rate for this stoichiometric methane/air flame is shown in Fig. 2. The experimental results from Taylor [25] and Gu et al. [22] are also plotted for comparison. It is seen that numerical prediction from A-SURF agrees well with the experimental results. There is some scatter in the experimental data, especially in those from Gu et al. [22]. This is caused by the fact that only limited points of the flame front history, $R = R(t)$, can be recorded in experiments and used for calculating the differentiation, dR/dt. The computed results are shown to be very smooth since enough points of the flame front history are readily available in simulation. Though a good linear fit between S_b and K can be obtained for both computed and measured results, the scatter in the experimental results can cause discrepancy in the fitted results for S_b^0 and L_b. The dashed lines in Fig. 2(b) show the flame radii contours (they are straight lines since $R = 2S_b/K$). It can be observed that extrapolations based on different flame radii ranges measured by experiments will give different fitted results.

Quantitatively, Table 1 shows the fitted values of S_b^0 and L_b using linear extrapolations based on two different flame radii ranges: $1.0 \le R \le 1.5$ cm and $1.5 \le R \le 2.0$ cm. For simulation, the relative difference between results from these two linear extrapolations for both S_b^0 and L_b is below 2%. However, for experiment, the relative difference for S_b^0 is below 5%, while

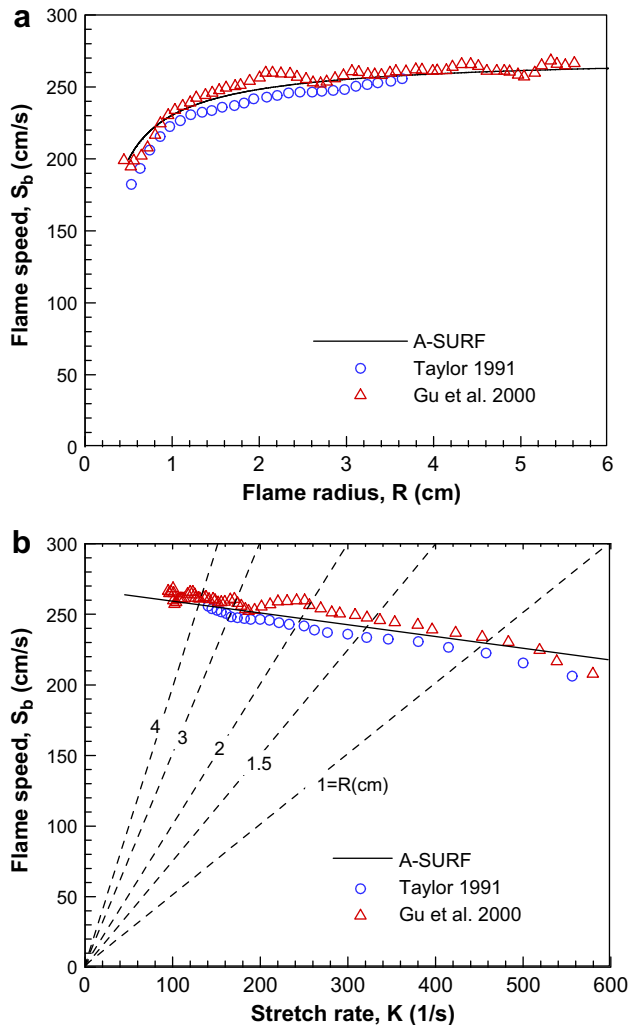

Fig. 2 – Computed (solid line) and measured (symbols) flame speed at different (a) flame radii and (b) stretch rates of a propagating stoichiometric methane/air flame at atmospheric pressure.

that for L_b is above 20%. Therefore, the computed laminar flame speed and Markstein length as well as the measured laminar flame speed are relatively insensitive to the flame radii range utilized for linear extrapolation, while the measured Markstein length strongly depends on the flame radii range utilized for data processing. Constrained by the chamber size and window size of experimental equipments, different groups usually conduct extrapolation based on different flame radii ranges [19]. As a result, good agreement among the laminar flame speeds measured by different researchers can be achieved while different values of L_b from experimental measurements will be reported.

The validity of the above statement is further demonstrated by Fig. 3, which shows S_u^0 and L_b changing with the equivalence ratio for atmospheric methane/air flames. Except for the laminar flame speed calculated by PREMIX (dash–dot line) [32], the experimental (symbols) and numerical (solid line) results were all obtained through the linear extrapolation of S_b and K based on the recorded flame front history of propagating spherical flames. As expected, Fig. 3(a) shows that the laminar flame speed from experiments is consistent with numerical prediction and the experimental results from different researchers agree well with each other, except for very lean methane/air flames whose laminar flame speed is below 10 cm/s and hence buoyancy effects are not negligible in experiments. However, unlike the laminar flame speed, Fig. 3(b) shows that there is a very large discrepancy for Markstein length measured by different researchers and the relative difference can even be larger than 300%. The Markstein length relative to burned gas measured by Halter et al. [6] is shown to be several times larger than those by Taylor [25], Gu et al. [22], and numerical simulation, especially for rich methane/air flames. (The so-called "burned gas Markstein length" shown in Fig. 6 of Ref. [6] is in fact the Markstein length relative to unburned gas. It is converted to L_b by multiplying the density ratio ρ_u/ρ_b.)

Therefore, according to results shown in Table 1, Figs. 2 and 3, the measurements of Markstein length have a very large uncertainty (~100%) since it is very sensitive to the flame radii range utilized for linear extrapolation. This problem can be solved with the help of numerical simulations of propagating spherical flames, which can accurately predict the Markstein length (the numerical uncertainties for the calculated Markstein length are below 5%), especially for methane/air and hydrogen/air flames whose chemical mechanism is well developed and extensively validated. In the following, the hydrogen blended methane/air flames will be studied and the laminar flame speed as well as Markstein length predicted by simulation will be presented and compared with experimental results in the literature [6–8].

3.2. *Effects of hydrogen addition*

Numerical simulations of propagating methane/air flames at different hydrogen blending levels ($a = 0$, 0.2, 0.4, 0.6, 0.8, 1), equivalence ratios ($\varphi = 0.8$, 1, 1.2), and pressures ($P = 0.8$, 1, 2 atm) are conducted using A-SURF.

Table 1 – Effects of flame radii range on the extrapolated S_b^0 and L_b.

Data range used for linear extrapolation	Experiment (Gu et al. [22])		Experiment (Taylor [25])		Simulation (A-SURF)	
	S_b^0 (cm/s)	L_b (mm)	S_b^0 (cm/s)	L_b (mm)	S_b^0 (cm/s)	L_b (mm)
1.0 cm ≤ R ≤ 1.5 cm	281.4	1.05	258.2	0.73	267.7	0.78
1.5 cm ≤ R ≤ 2.0 cm	288.2	1.27	269.2	1.11	268.4	0.79
Relative difference	2.4%	21.0%	4.3%	52.1%	0.3%	1.3%

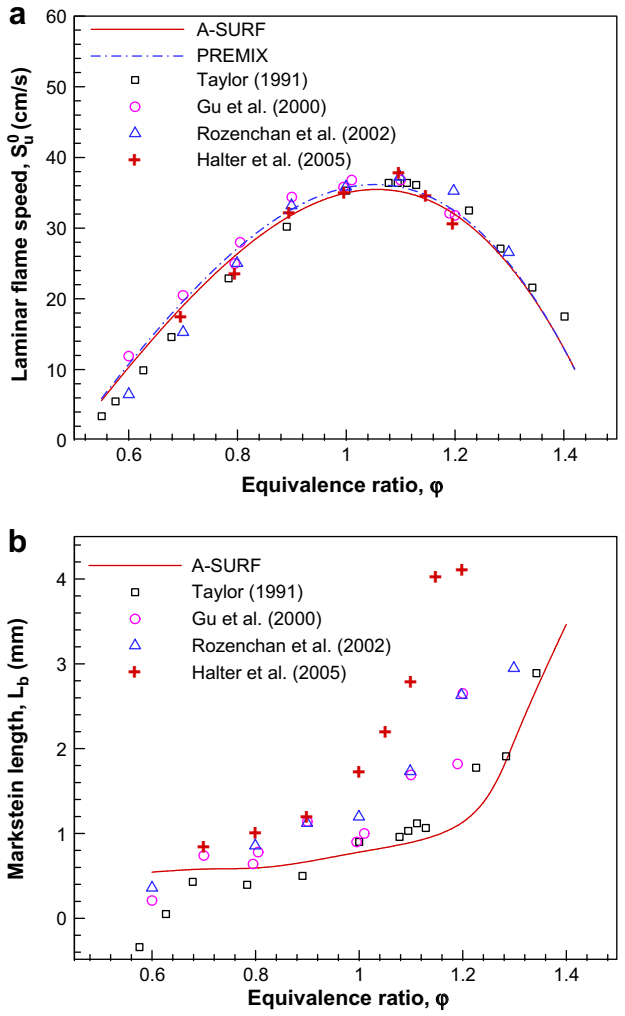

Fig. 3 – (a) Laminar flame speed and (b) Markstein length relative to burned gas of atmospheric methane/air flames (symbols: measured values; lines: computed values).

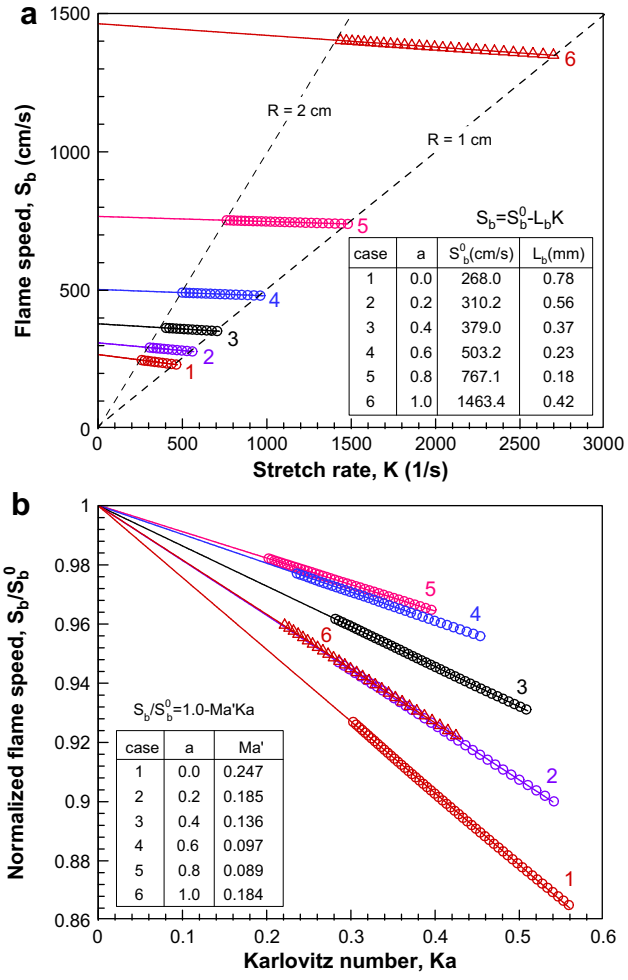

Fig. 4 – (a) S_b versus K; (b) S_b/S_b^0 versus Ka for stoichiometric methane/hydrogen/air flames at atmospheric pressure (symbols: computed values; solid lines: linear extrapolation).

Fig. 4 shows the results for stoichiometric methane/hydrogen/air flames at atmospheric pressure. The relationships between flame speed and stretch rate in dimensional and non-dimensional forms are shown by Fig. 4(a) and (b), respectively. Only the computed data of flame radius between $R=1$ cm and $R=2$ cm are presented since in simulation the extrapolated results of S_b^0 and L_b are insensitive to the flame radii range. Moreover, this flame radii range is close to those used in experiments [5–8,22–25]. As expected, Fig. 4(a) shows that flame speed and stretch rate both increase with hydrogen addition. The enhancement of flame speed by hydrogen addition is due to an increase in the flame temperature (thermal effect) and a decrease of chemical activation energy (chemical effect) [2]. It is also seen that the stretched flame speed decreases with stretch rate at a similar trend for all the hydrogen blending levels. Therefore, the Markstein length/number is always positive.

Using the linear extrapolation based on Eq. (1) or (2), the values of S_b^0, L_b, and Ma', can be determined. The results are presented in the tables inserted in Fig. 4 and are also shown in Fig. 5. It is seen that S_b^0 increases monotonically with hydrogen addition (due to thermal and chemical effects mentioned before), while L_b and Ma' changes non-monotonically with hydrogen blending: they first decrease and then increase. On one hand, blending of hydrogen to pure methane/air results in a decrease in L_b and Ma' and consequently promotes the diffusive-thermal instability. This agrees with experimental observations by Miao et al. [8] who showed that surface cellular instability of propagating spherical methane/hydrogen/air flames occurs earlier when more hydrogen is added. On the other hand, blending of methane to pure hydrogen/air also decreases L_b and Ma' and hence destabilizes the flame. This destabilizing effect of methane on hydrogen was confirmed in experiments of propagating spherical methane/hydrogen/air flames by Law and Kwon [5]. Therefore, the non-monotonic behavior predicted by simulation is consistent with experimental observations of propagating spherical flames. Besides spherical flames, the same non-monotonic variation of Markstein length with hydrogen blending was also reported for lean methane/hydrogen/air counterflow flames [13]. The non-monotonic behavior was

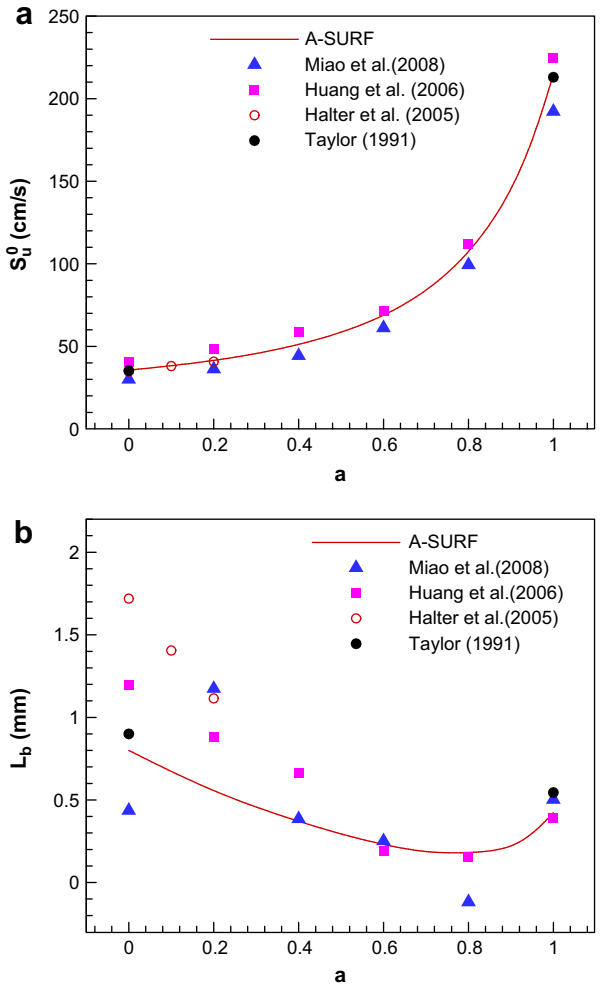

Fig. 5 – (a) Laminar flame speed and (b) Markstein length relative to burned gas of stoichiometric methane/hydrogen/air flames at atmospheric pressure (symbols: measured values; lines: computed values).

explained [13] using the following expression derived from asymptotic analysis [15]

$$\frac{L_b}{\delta^0} = \frac{\ln(1/\sigma)}{1-\sigma} + \frac{Ze(Le-1)}{2}\frac{1}{1-\sigma}\int_0^{(1/\sigma)-1}\frac{\ln(1+x)}{x}dx \qquad (3)$$

where Le is the Lewis number and Ze is the Zel'dovich number. With the addition of hydrogen, both Le (<1.0) and Ze decrease, which results in a non-monotonic change of Ze(1 – Le). The competing effects of Le and Ze were claimed to be responsible for the non-monotonic change of Markstein length with hydrogen blending [13].

Fig. 5 shows the comparison of the computed and measured unstretched laminar flame speed and Markstein length for stoichiometric methane/hydrogen/air flames (note that natural gas instead of methane is used in the experiments by Huang and coworkers [7,8]). It is seen that good agreement among laminar flame speeds measured by different researchers and computed from simulations (computed laminar flame speed via PREMIX is found to be nearly identical to that via A-SURF and hence is not shown) is achieved except that for pure hydrogen/air flames ($a = 1$). However, for the Markstein length shown in Fig. 5(b), the relative difference among measured results by different researchers is in the order of 100% and the non-monotonic change of Markstein length with hydrogen blending is not captured by Miao et al. [8]. As mentioned before, this is because the measured laminar flame speed is relatively insensitive to the flame radii range utilized for linear extrapolation while the measured Markstein length relative to burned gas strongly depends on the flame radii range utilized for data processing and different groups usually conduct extrapolation based on different flame radii ranges. Due to the large uncertainty in experimental measurements, the measured Markstein length is not reliable. The computed one is much more accurate and hence should be used in combustion modeling considering the flame stretch effect on flame speed.

Besides the stoichiometric case, both lean ($\varphi = 0.8$) and rich ($\varphi = 1.2$) methane/hydrogen/air flames at atmospheric pressure are studied and the results are shown in Figs. 6–9. For fuel lean case, Fig. 6 shows that flame speed and stretch rate both increase with the amount of hydrogen blending which is

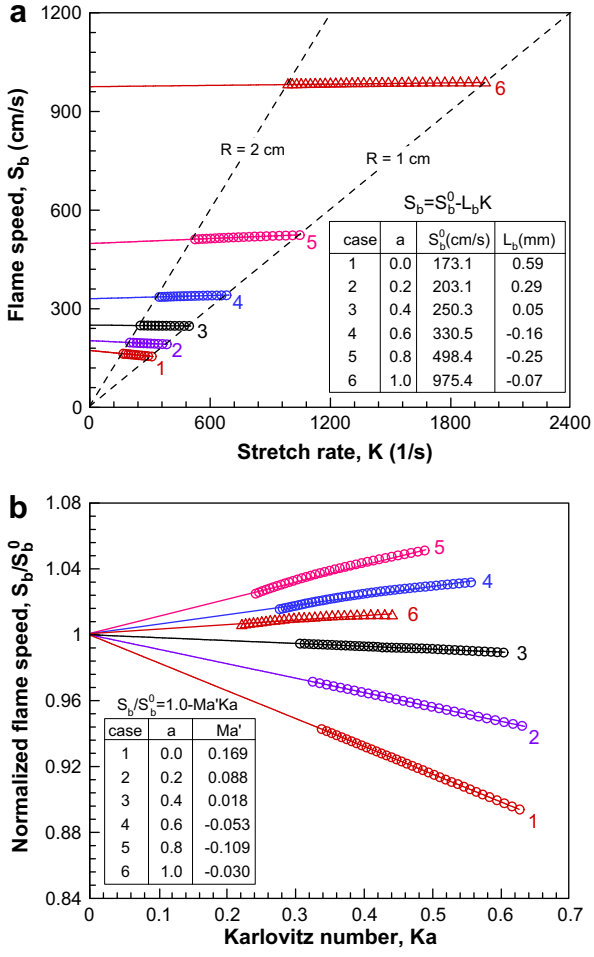

Fig. 6 – (a) S_b versus K; (b) S_b/S_b^0 versus Ka for lean ($\varphi = 0.8$) methane/hydrogen/air flames at atmospheric pressure (symbols: computed values; solid lines: linear extrapolation).

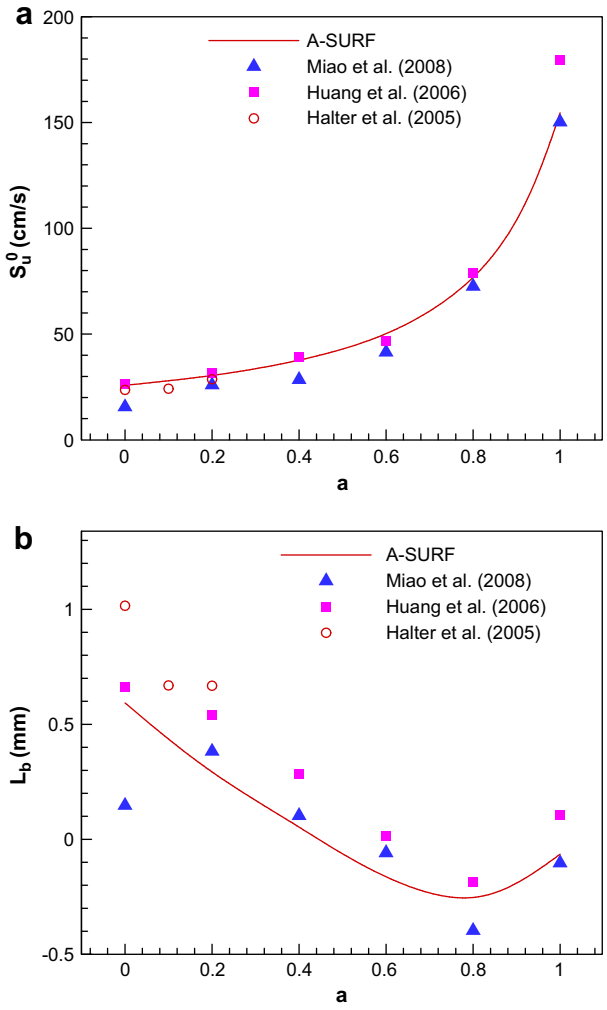

Fig. 7 – (a) Laminar flame speed and (b) Markstein length relative to burned gas of lean (φ = 0.8) methane/hydrogen/air flames at atmospheric pressure (symbols: measured values; lines: computed values).

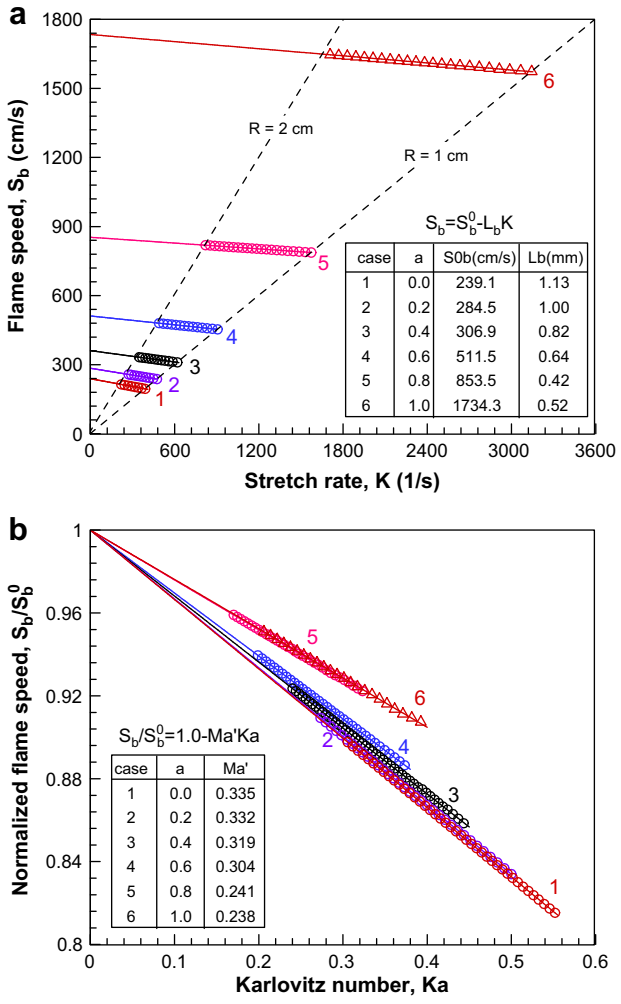

Fig. 8 – (a) S_b versus K; (b) S_b/S_b^0 versus Ka for rich (φ = 1.2) methane/hydrogen/air flames at atmospheric pressure (symbols: computed values; solid lines: linear extrapolation).

similar to the trend of the stoichiometric case. However, unlike the results for $\varphi = 1.0$ shown in Fig. 4, Fig. 6 shows that the stretched flame speed does not decrease with stretch rate for all the hydrogen blending levels. As shown by the tables inserted in Fig. 6, L_b and Ma' becomes negative for $a = 0.6$, 0.8 and 1.0, which means that the stretched flame speed increases with stretch rate. (Note that for $a = 0.6$, 0.8 and 1.0, there is a non-linear trend between S_b/S_b^0 and Ka. The accuracy of the laminar flame speed and Markstein length from linear extrapolation is decreased due to the non-linear effect [36].) This is because when hydrogen dominates in the lean dual fuel, the Lewis number of the mixture is lower than the critical Lewis number for which the flame stretch effect is zero, and the positive flame stretch thus makes the flame stronger than the unstretched planar flame [16]. However, for the fuel rich case, Fig. 8 shows that the stretched flame speed always decreases with stretch rate for all the hydrogen blending levels. This is because the Lewis number of the rich methane/hydrogen/air mixture is higher than the critical Lewis number. Comparison of the Markstein length shown by tables in Figs. 4, 6, and 8 for $\varphi = 0.8$, 1.0, and 1.2, respectively, shows that the Markstein length (and thus the Lewis number and the flame stability) of methane/hydrogen/air increases with the equivalence ratio. This is consistent with results from previous studies on pure methane/air and pure hydrogen/air flames [16,25].

The computed and measured unstretched laminar flame speed and Markstein length for lean and rich methane/hydrogen/air flames are shown in Figs. 7 and 9, respectively. Similar to the results for the stoichiometric case, the laminar flame speed increases monotonically while the Markstein length changes non-monotonically with hydrogen blending. Figs. 7 and 9 also show good agreement among laminar flame speeds measured by different researchers and predicted by numerical simulation. However, a very large discrepancy is shown for Markstein length measured by different researchers. Therefore the measured Markstein length has a very large uncertainty and is not accurate.

Hydrogen blended methane/air flames at subatmospheric pressure ($P = 0.8$ atm) and elevated pressure ($P = 2$ atm) are

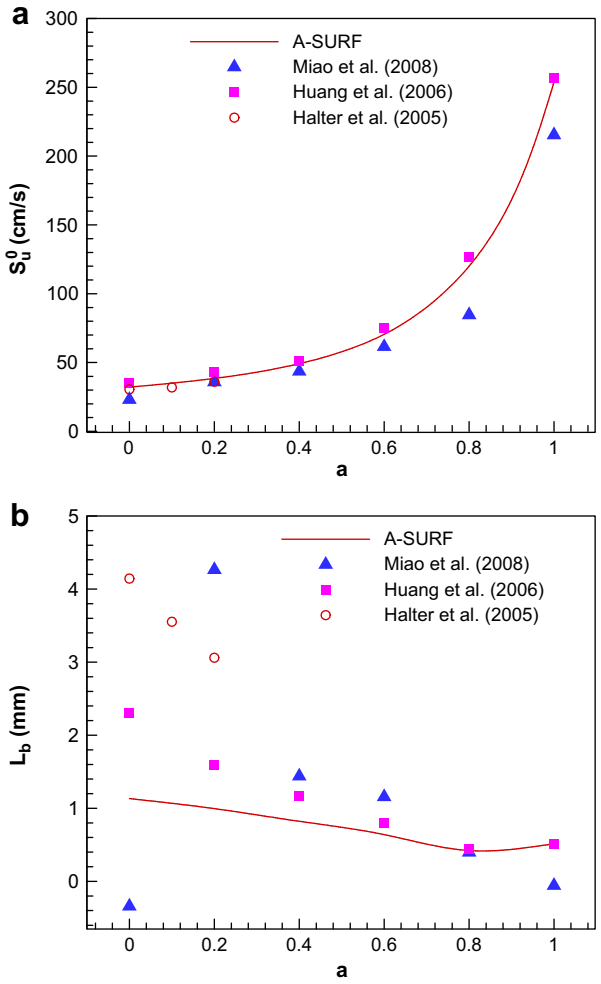

Fig. 9 – (a) Laminar flame speed and (b) Markstein length relative to burned gas of rich ($\varphi = 1.2$) methane/hydrogen/air flames at atmospheric pressure (symbols: measured values; lines: computed values).

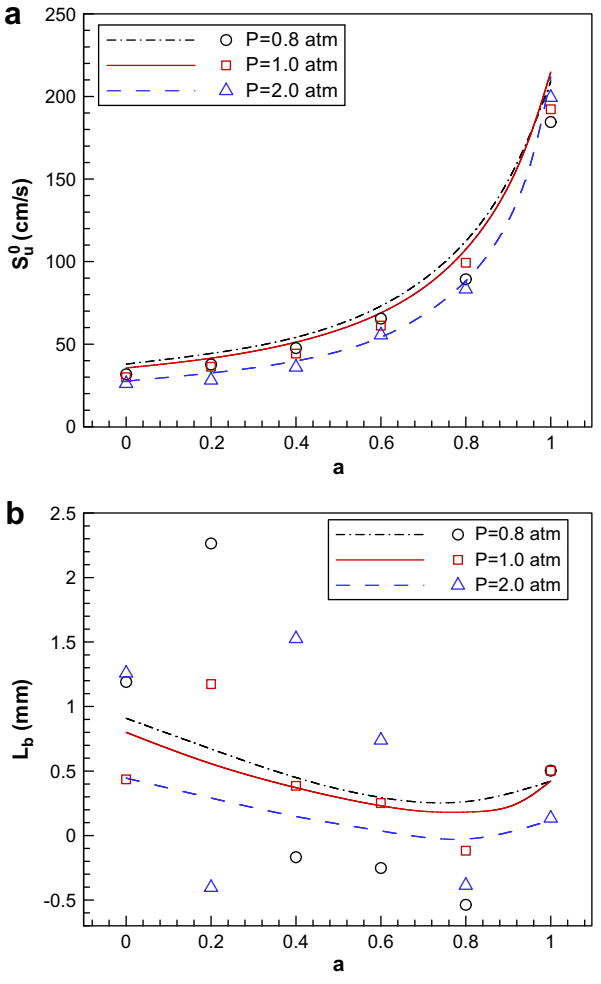

Fig. 10 – (a) Laminar flame speed and (b) Markstein length relative to burned gas of stoichiometric methane/hydrogen/air flames at different hydrogen blending levels and pressures (symbols: measured values from Miao et al. [8]; lines: computed values).

also investigated. It is found that flame speed and stretch rate both increase with the amount of hydrogen blending, and that the stretched flame speed always decreases with stretch rate for all the hydrogen blending levels (thus L_b is always positive). The laminar flame speed and Markstein length from simulations via A-SURF and experiments by Miao et al. [8] are shown in Fig. 10. It is seen that the laminar flame speed decreases with pressure when the hydrogen blending level is below $a < 0.9$, while it increases with pressure when a is close to unity (i.e. for hydrogen/air without or with a very small amount of methane addition). The dependence of laminar flame speed on pressure is determined by the overall reaction order through $S_u^0 \sim P^{n/2-1}$. The overall reaction order, n, of a stoichiometric methane/air flame around atmospheric pressure is about 1.5 [16] and hence S_u^0 decreases with P; while that of a stoichiometric hydrogen/air flame around atmospheric pressure is slightly above 2.0 [16] and hence S_u^0 increases with P. It is seen that the experimental measurements [8] accurately captured the trend of S_u^0 changing with P for methane/hydrogen/air flames.

For Markstein length, Fig. 10(b) shows that the computed Markstein length changes non-monotonically with hydrogen blending for all the pressures studied and that the computed Markstein length decreases with pressure for all the hydrogen blending levels. The change due to pressure can also be explained by using the asymptotic result on Markstein length given by Eq. (3). With the increase of pressure, the flame thickness (δ^0) decreases while the change of Lewis number (Le), Zel'dovich number (Ze), and density ratio (σ) is negligible for $0.8 \le P \le 2$ atm [16]. Consequently, according to Eq. (3), the Markstein length (L_b) decreases with pressure and hence the dependence of the flame speed on stretch rate becomes weaker at higher pressure. Fig. 10(b) shows very large scatter in the measured Markstein length. The measured results do not show the non-monotonic behavior of L_b changing with hydrogen blending for a specific pressure, nor do they show the trend that L_b decreases with pressure for a specific blending level. In fact, it is seen that the measured L_b increases with pressure for blending level of $a = 0.4$ and $a = 0.6$, which is not correct. Therefore, the experimentally measured

Markstein length has a large uncertainty and cannot be used to characterize the dependence of the stretched flame speed on flame stretch rate. On the other hand, the computed Markstein length is much more accurate and is suitable for application in combustion modeling considering the flame stretch effect on flame speed.

4. Conclusions

High-fidelity numerical simulations of propagating spherical methane/air flames at different hydrogen blending levels, equivalence ratios, and pressures are conducted. The effects of hydrogen addition on the flame propagating speed and Markstein length are systematically investigated. The computed results are compared with measured data in the literature. The main conclusions are:

(1) The stretched and unstretched laminar flame speeds as well as stretch rate increase monotonically with the amount of hydrogen blending. However, the Markstein length, which characterizes the dependence of the flame propagating speed on stretch rate and cellular instability of propagating flames, is shown to change non-monotonically with hydrogen blending: blending of hydrogen to methane/air and blending methane to hydrogen/air both can decrease the Markstein length and thus destabilize the flame. A similar trend of flame speed and Markstein length changing with hydrogen addition is observed for all the equivalence ratios and pressures considered in this study.
(2) The computed laminar flame speed and Markstein length as well as the measured laminar flame speed are found to be relatively insensitive to the flame radii range utilized for linear extrapolation, while the measured Markstein length relative to burned gas strongly depends on the flame radii range. Consequently, good agreement among laminar flame speeds measured by different researchers and predicted by simulations is achieved. However, the experimentally measured Markstein length has very large uncertainty (~100%) and cannot correctly show the trend of Markstein length changing with the hydrogen blending level and pressure. Therefore, the measured Markstein length is not reliable, and the computed one is much more accurate and should be used in combustion modeling considering the flame stretch effect on flame speed.

Acknowledgments

This work was partially supported by the research fund from State Key Laboratory for Turbulence and Complex Systems and the start-up fund from Peking University.

REFERENCES

[1] Fotache CG, Kreutz TG, Law CK. Ignition of hydrogen-enriched methane by heated air. Combustion and Flame 1997;110:429–40.
[2] Yu G, Law CK, Wu CK. Laminar flame speeds of hydrocarbon + air mixtures with hydrogen addition. Combustion and Flame 1986;63:339–47.
[3] Shrestha SOB, Karim GA. Hydrogen as an additive to methane for spark ignition engine applications. International Journal of Hydrogen Energy 1999;24:577–86.
[4] Bauer CG, Forest TW. Effect of hydrogen addition on the performance of methane-fueled vehicles. Part I: effect on SI engine performance. International Journal of Hydrogen Energy 2001;26:55–70.
[5] Law CK, Kwon OC. Effects of hydrocarbon substitution on atmospheric hydrogen–air flame propagation. International Journal of Hydrogen Energy 2004;29:867–79.
[6] Halter F, Chauveau C, Djeballi-Chaumeix N, Gokalp I. Characterization of the effects of pressure and hydrogen concentration on laminar burning velocities of methane–hydrogen–air mixtures. Proceedings of the Combustion Institute 2005;30:201–8.
[7] Huang Z, Zhang Y, Zeng K, Liu B, Wang Q, Jiang DM. Measurements of laminar burning velocities for natural gas–hydrogen–air mixtures. Combustion and Flame 2006;146:302–11.
[8] Miao HY, Jiao Q, Huang ZH, Jiang DM. Effect of initial pressure on laminar combustion characteristics of hydrogen enriched natural gas. International Journal of Hydrogen Energy 2008;33:3876–85.
[9] Jackson GS, Sai R, Plaia JM, Boggs CM, Kiger KT. Influence of H_2 on the response of lean premixed CH_4 flames to high strained flows. Combustion and Flame 2003;132:503–11.
[10] Di Sarli V, Di Benedetto A. Laminar burning velocity of hydrogen–methane/air premixed flames. International Journal of Hydrogen Energy 2007;32:637–46.
[11] Wang JH, Huang ZH, Tang CL, Miao HY, Wang XB. Numerical study of the effect of hydrogen addition on methane–air mixtures combustion. International Journal of Hydrogen Energy 2009;34:1084–96.
[12] Guo HS, Smallwood GJ, Liu FS, Ju YG, Gulder OL. The effect of hydrogen addition on flammability limit and NOx emission in ultra-lean counterflow CH_4/air premixed flames. Proceedings of the Combustion Institute 2005;30:303–11.
[13] Sankaran R, Im HG. Effects of hydrogen addition on the Markstein length and flammability limit of stretched methane/air premixed flames. Combustion Science and Technology 2006;178:1585–611.
[14] Zhang YY, Wu JH, Ishizuka S. Hydrogen addition effect on laminar burning velocity, flame temperature and flame stability of a planar and a curved CH_4–H_2–air premixed flame. International Journal of Hydrogen Energy 2009;34:519–27.
[15] Clavin P. Dynamic behavior of premixed flame fronts in laminar and turbulent flows. Progress in Energy and Combustion Science 1985;11:1–59.
[16] Law CK. Combustion physics. Cambridge University Press; 2006.
[17] Markstein GH. Nonsteady flame propagation. Pergamon Press; 1964.
[18] Peters N. Turbulent combustion. New York: Cambridge University Press; 2000.
[19] Chen Z, Burke MP, Ju YG. Effects of compression and stretch on the determination of laminar flame speed using propagating spherical flames. Combustion Theory and Modelling 2009;13:343–64.
[20] Chen Z, Burke MP, Ju YG. Effects of Lewis number and ignition energy on the determination of laminar flame speed using propagating spherical flames. Proceedings of the Combustion Institute 2009;32:1253–60.
[21] Burke MP, Chen Z, Ju YG, Dryer FL. Effect of cylindrical confinement on the determination of laminar flame speeds using propagating spherical flames. Combustion and Flame 2009;156:771–9.

[22] Gu XJ, Haq MZ, Lawes M, Woolley R. Laminar burning velocity and Markstein lengths of methane–air mixtures. Combustion and Flame 2000;121:41–58.
[23] Rozenchan G, Zhu DL, Law CK, Tse SD. Outward propagation, burning velocities, and chemical effects of methane flames up to 60 atm. Proceedings of the Combustion Institute 2003;29:1461–70.
[24] Chen Z, Qin X, Ju YG, Zhao ZW, Chaos M, Dryer FL. High temperature ignition and combustion enhancement by dimethyl ether addition to methane–air mixtures. Proceedings of the Combustion Institute 2007;31:1215–22.
[25] Taylor SC. Burning velocity and the influence of flame stretch. Ph.D. Thesis, University of Leeds; 1991.
[26] Chen Z, Qin M, Xu B, Ju YG, Liu FS. Studies of radiation absorption on flame speed and flammability limit of CO_2 diluted methane flames at elevated pressures. Proceedings of the Combustion Institute 2007;31:2693–700.
[27] Chen Z. Studies on the initiation, propagation, and extinction of premixed flames. Ph.D. Thesis, Princeton University; 2009.
[28] Strang G. On the construction and comparison of difference schemes. SIAM Journal on Numerical Analysis 1968;5:506–17.
[29] Brown PN, Byrne GD, Hindmarsh AC. VODE: a variable-coefficient ODE solver. SIAM Journal on Scientific and Statistical Computing 1989;10:1038–51.
[30] Smith GP, Golden DM, Frenklach M, Moriarty NW, Eiteneer B, Goldenberg M, et al. http://www.me.berkeley.edu/gri_mech/.
[31] Kee RJ, Rupley FM, Miller JA. Chemkin-II: a FORTRAN package for the analysis of gas-phase chemical kinetics. Sandia National Laboratory report SAND89-8009B; 1989.
[32] Kee RJ, Grcar JF, Smooke MD, Miller JA. A FORTRAN program for modeling steady laminar one-dimensional premixed flames. Sandia National Laboratory report SAND85-8240; 1985.
[33] Bradley D, Gaskell PH, Gu XJ. Burning velocities, Markstein lengths, and flame quenching for spherical methane–air flames: a computational study. Combustion and Flame 1996; 104:176–98.
[34] Chen Z, Ju Y. Theoretical analysis of the evolution from ignition kernel to flame ball and planar flame. Combustion Theory and Modelling 2007;11:427–53.
[35] Qiao L, Kim CH, Faeth GM. Suppression effects of diluents on laminar premixed hydrogen/oxygen/nitrogen flames. Combustion and Flame 2005;143:79–96.
[36] Kelly AP, Law CK. Nonlinear effects in the experimental determination of laminar flame properties from stretched flames. Fall technical meeting: eastern states sections of the Combustion Institute, Virginia, paper B-11; 2007.